Click Here for Full Article

Midnight temperature maximum (MTM) in Whole Atmosphere Model (WAM) simulations

R. A. Akmaev,[1] F. Wu,[2] T. J. Fuller-Rowell,[2] and H. Wang[2]

[1] Discovered almost four decades ago, the midnight temperature maximum (MTM) with typical magnitudes of 50–100 K has been regularly observed by satellite and ground-based instruments in the tropical upper thermosphere. Although several mechanisms have been suggested to explain the phenomenon, previous attempts to reproduce it with comprehensive thermosphere-ionosphere models have been unsuccessful. First long-term simulations with the Whole Atmosphere Model (WAM) reveal the presence of a realistically prominent MTM and reproduce the salient features of its daily, seasonal, and latitudinal variability. Preliminary analysis indicates that the feature may be traced down to the lower thermosphere, where it is manifested primarily in the form of an upward propagating terdiurnal tidal wave. Its spectrum expands to higher-order zonal wavenumbers and frequencies and its phase advances to near midnight higher up in the thermosphere. Possible mechanisms generating this wave may involve nonlinear interactions between other tidal harmonics originating in the middle and lower atmosphere. Our results thus suggest that the MTM is yet another phenomenon driven by dynamical links between the lower and upper atmosphere and ionosphere. **Citation:** Akmaev, R. A., F. Wu, T. J. Fuller-Rowell, and H. Wang (2009), Midnight temperature maximum (MTM) in Whole Atmosphere Model (WAM) simulations, *Geophys. Res. Lett.*, *36*, L07108, doi:10.1029/2009GL037759.

1. Introduction

[2] The MTM was first reported in radar measurements of ion temperature in the thermosphere over Arecibo (18°N) in the early 1970s [*Harper*, 1973]. In 1977–1978 systematic observations were made at low latitudes equatorward of ±20° by the Neutral Atmosphere Temperature Experiment (NATE) instrument on the Atmosphere Explorer-E (AE-E) satellite [*Spencer et al.*, 1979]. An AE-E climatology describing seasonal and horizontal variations of the MTM was compiled in an altitude range of 250–370 km for this period of low solar activity [*Herrero and Spencer*, 1982]. It is generally consistent with ground-based optical observations, primarily in the tropical American sector, often indicating a poleward propagation of the feature with typical magnitudes of about 50–100 K around midnight [e.g., *Faivre et al.*, 2006]. Recent observations of a nightglow brightness wave, commonly associated with the MTM, suggest that the phenomenon may also extend into mid-latitudes [*Colerico et al.*, 2006].

[3] *Mayr et al.* [1979] found a substantial terdiurnal component in the AE-E measurements, particularly on days of a prominent MTM. They advanced a mechanism whereby the terdiurnal and possibly higher harmonics are generated in situ by nonlinear interactions between the semidiurnal tide propagating from the lower atmosphere and the diurnally varying ion drag. It therefore remains somewhat of a mystery that subsequent attempts to reproduce a realistic MTM in coupled ionosphere-thermosphere models, which include all the relevant physical processes, have been unsuccessful even after substantial adjustments of amplitudes and phases of the semidiurnal tidal modes [*Fuller-Rowell*, 1981; *Fesen*, 1996; *Meriwether et al.*, 2008]. It has been suggested that higher-order tidal harmonics entering the thermosphere from below may be needed to produce a realistic MTM in these models [e.g., *Colerico et al.*, 2006].

2. Model

[4] The Whole Atmosphere Model (WAM) is being developed under the Integrated Dynamics in the Earth's Atmosphere (IDEA) project to study dynamical links between the lower atmosphere and the upper atmosphere and ionosphere [*Akmaev et al.*, 2008; *Akmaev and Juang*, 2008; *Fuller-Rowell et al.*, 2008]. It represents a neutral-atmosphere component of the coupled IDEA model and is an extension of the medium-range weather prediction Global Forecast System (GFS) model to the top of the atmosphere [*Akmaev et al.*, 2008].

[5] Several long free-running (i.e., without constraints imposed by data assimilation) simulations have been conducted to evaluate the model's climatology and internal variability. The model was run for 15 months and the output was analyzed for the last 12 months. Here we present a preliminary analysis of the MTM found in the simulations for low solar activity and quiet geomagnetic conditions.

3. Results and Discussion

[6] Figure 1 presents snapshots of temperature deviation ΔT from the zonal mean T_0 at a pressure level near 285 km in March at 20°N (top) and December at 30°S (bottom). Each thin line represents one day in a given month, and the two columns correspond to two different UT-longitude sectors. A prominent MTM with a magnitude between about 50 K and well over 100 K clearly stands out at both locations and seasons. Strong day-to-day variability is also evident, not unlike the variability observed from AE-E [*Spencer et al.*, 1979]. An MTM is invariably seen in other seasons at low- to mid-latitudes in the upper thermosphere

---

[1]Space Weather Prediction Center, NOAA, Boulder, Colorado, USA.
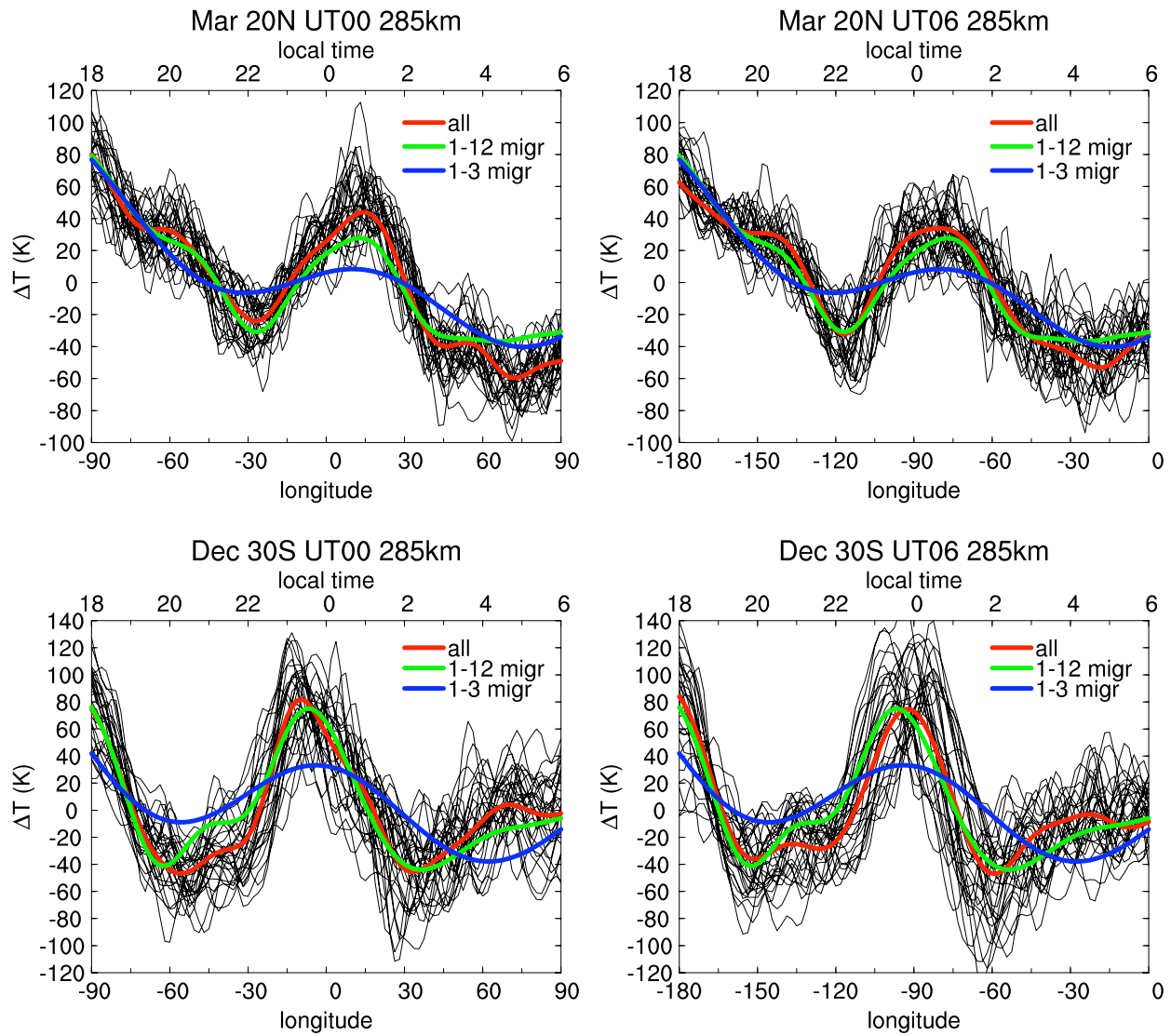[2]CIRES, University of Colorado, Boulder, Colorado, USA.

Figure 1. Temperature deviation from the zonal mean near 285 km in (top) March at 20°N and (bottom) December at 30°S at (left) UT = 0:00 and (right) UT = 6:00. See text for details.

(for a sample horizontal structure see Figure 5), sometimes exhibiting more variability in the time of occurrence and smaller magnitudes. In agreement with the analysis of *Herrero and Spencer* [1982], at a given height the magnitude is typically largest in summer (e.g., Figure 1, bottom), and it continues to increase with height in most locations.

[7] A substantial part of the internally generated variability seen in Figure 1 is clearly driven by waves at relatively small scales. The thermosphere is a naturally strongly dissipative medium, eliminating the need for "sponge layers" and extra numerical dissipation often imposed in upper layers to stabilize atmospheric model codes. WAM employs no "sponge layers" and remains stable using a substantially reduced numerical Rayleigh friction coefficient even compared to the standard version of GFS [*Akmaev et al.*, 2008]. Numerical experiments show that both the size of the MTM and especially its variability are very sensitive to imposed numerical dissipation. Excessive numerical dissipation [*Sutton*, 2008] and perhaps insufficient horizontal and vertical resolution may be some of the
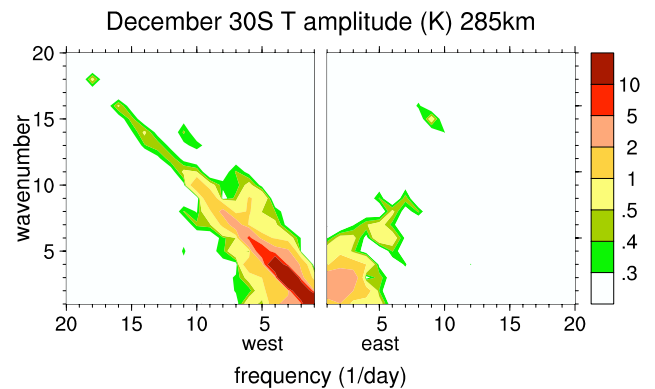

Figure 2. Temperature amplitude spectrum as a function of frequency and zonal wavenumber for December at 30°S near 285 km. Westward migrating waves are located on the diagonal of the left plot.
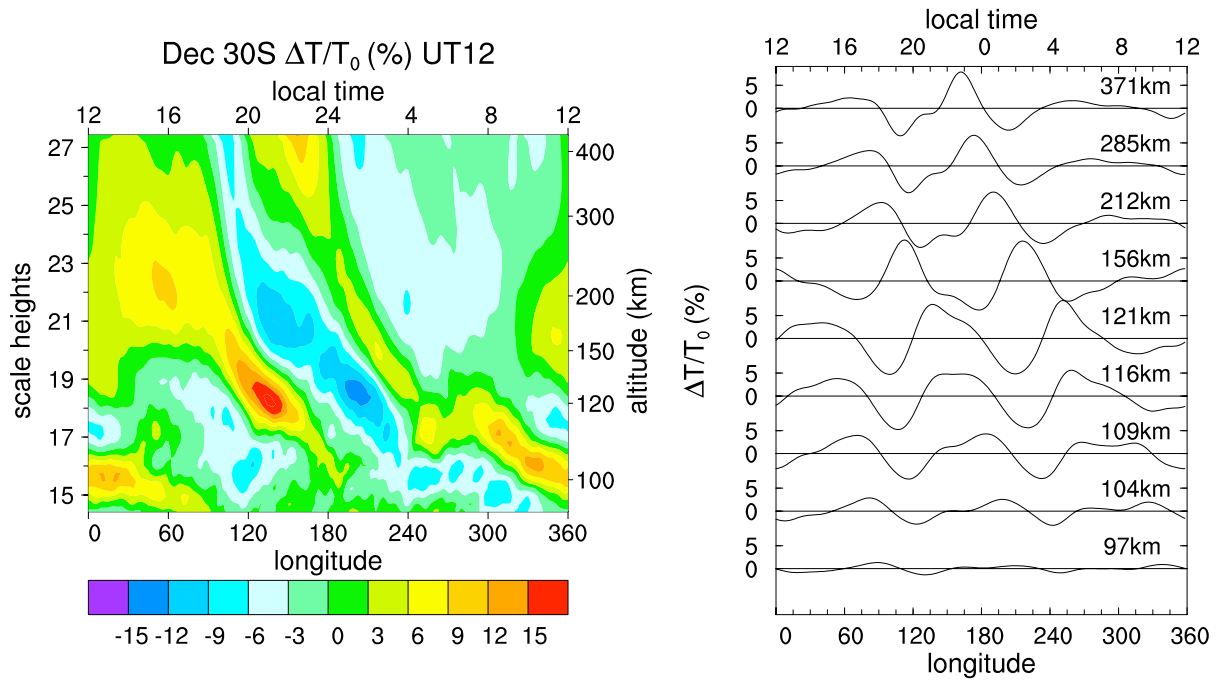
Figure 3. (left) Relative temperature deviation as a function of height and longitude (local time) for December at 30°S and UT = 12:00. (right) The same signal reconstructed using migrating waves with zonal wavenumbers 3–12 at select levels.

reasons for the inability of previous models to generate a realistic MTM.

[8] The whole feature migrates to the west following the apparent motion of the sun but substantial UT-longitude variability is also evident suggesting a contribution from non-migrating waves at various scales. A double Fourier analysis in time and longitude [*Akmaev et al.*, 2008] reveals a spectrum consisting of non-migrating waves propagating both eastward and westward in addition to the migrating waves (Figure 2). Following the spectrum from the lower thermosphere shows an expansion with altitude of the tail of westward migrating waves to higher frequencies and zonal wavenumbers along the diagonal in Figure 2 (left). These waves form the bulk of the MTM feature as illustrated by

the green lines in Figure 1 presenting a monthly mean reconstruction of the signal by migrating waves up to zonal wavenumber 12. The blue lines represent a sum of the first three migrating tidal harmonics, suggesting that the terdiurnal tide alone is not sufficient for a realistically sized MTM. The red lines sum up all waves in the double Fourier spectrum up to zonal wavenumber 12 and frequency 12 day^{-1} (period 2 hours). These are a good representation of the monthly mean signal and also reproduce the UT-longitude variability due to non-migrating waves.

[9] Figure 3 presents a monthly mean relative temperature deviation $\Delta T/T_0$ as a function of altitude and longitude for December at 30°S and UT = 12:00 (Figure 3, left). It shows how a three-peak (terdiurnal) structure emerges from
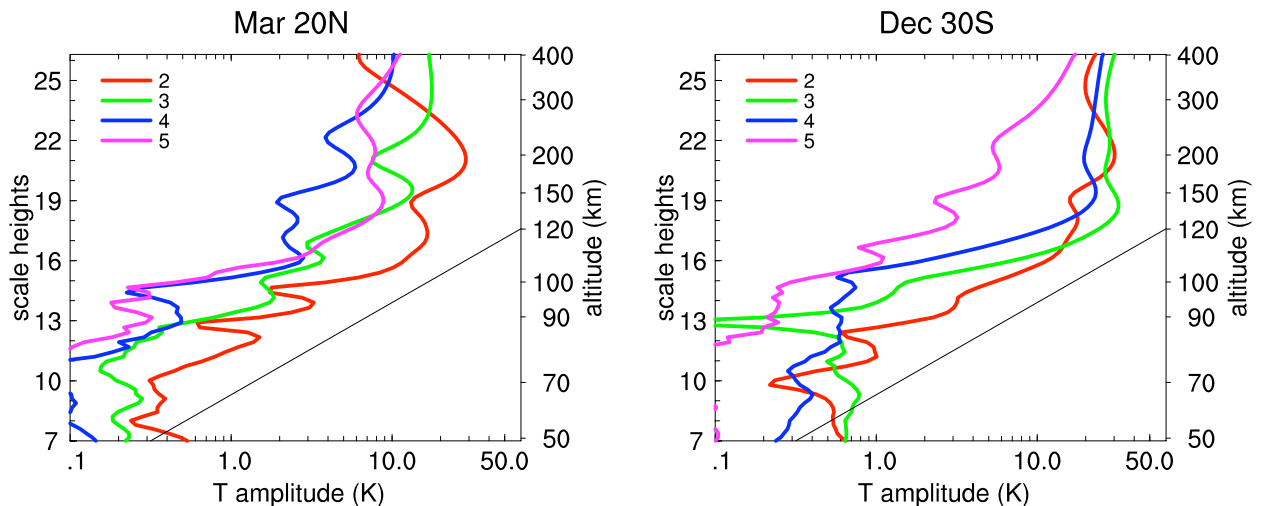

Figure 4. Monthly mean temperature amplitudes of migrating waves with zonal wavenumbers 2–5 as a function of height for (left) March at 20°N and (right) December at 30°S. The thin straight lines approximately show the altitude dependence for conservative waves.
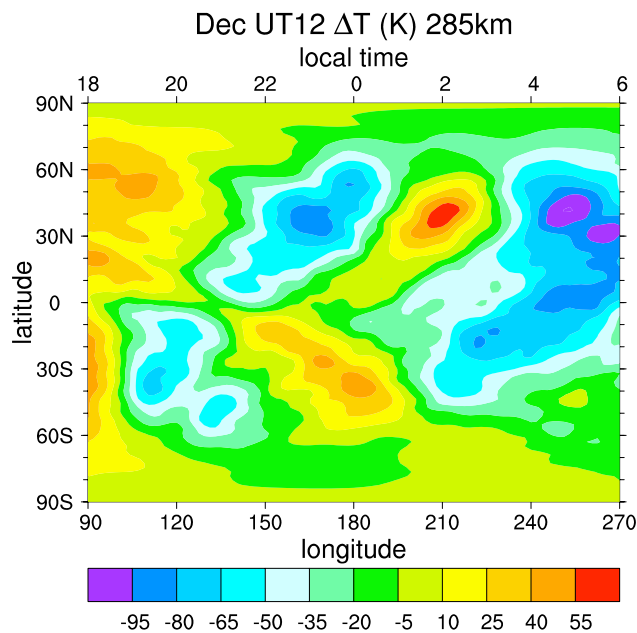
Dec UT12 ΔT (K) 285km

Figure 5. Monthly mean temperature deviation from the zonal mean in December near 285 km at UT = 12:00 as a function of latitude and longitude (local time).

a predominantly semidiurnal variation above about 100 km. As it propagates upward, the phase (time of maximum) of one of the three temperature maxima advances from morning hours to near midnight. This is also illustrated in Figure 3 (right) presenting a reconstruction of the signal by migrating waves with zonal wavenumbers 3–12 at select altitudes. As the three-peak structure propagates upward and its phase advances to earlier times, two of the three maxima appear to be suppressed by enhanced dissipation during daytime and only the nighttime maximum survives at a substantial magnitude, which is conceptually similar to the mechanism proposed by *Mayr et al.* [1979].

[10] The rapid emergence of a strong terdiurnal tide in the lower thermosphere deserves further investigation. However, it is already clear from a preliminary analysis (Figure 4) that only a relatively small fraction of this tide arrives from below while the bulk of the oscillation is likely generated in situ in the lower thermosphere. This is evidenced by the fast amplitude growth of the terdiurnal wave with altitude as well as its phase discontinuities (not shown) at the base of the thermosphere. As is well known, the gravest mode of the terdiurnal tide is evanescent in the mesosphere because of the negative temperature lapse rate [e.g., *Akmaev*, 2001]. In the thermosphere this mode can again propagate freely and grow exponentially with height (Figure 4). Several mechanisms may contribute to its generation here including direct solar radiative forcing and nonlinear interactions between the diurnal and semidiurnal tides [*Akmaev*, 2001], as well as possibly nonlinear interactions between the semidiurnal tide and ion drag [*Mayr et al.*, 1979]. Relative contributions of the different generation mechanisms can only be determined by a further in-depth analysis of the respective forcing terms.

[11] Higher-order migrating harmonics also begin to grow rapidly after the terdiurnal wave attains a substantial

amplitude (Figure 4). The extension of the spectral tail of migrating waves (Figure 2, left) most likely represents a spectral manifestation of the selective damping of the initial predominantly terdiurnal wave during daytime as it propagates upward [e.g., *Bracewell*, 2000]. As already mentioned above, this is conceptually consistent with the mechanism of *Mayr et al.* [1979] but applied to migrating harmonics of higher order, not just the semidiurnal tide.

[12] Figure 5 presents a horizontal structure of ΔT near 285 km in December, which is consistent with the AE-E climatology at solstice conditions [*Herrero and Spencer*, 1982], including the common observation that in summer the tropical MTM peaks earlier and attains larger magnitudes than in winter [e.g., *Faivre et al.*, 2006]. As the V-shape structure depicted in Figure 5 migrates westward, the MTM will appear moving poleward to an observer on the ground [*Herrero and Spencer*, 1982; *Meriwether et al.*, 2008]. Our simulations also show the MTM extend well into mid-latitudes [cf. *Colerico et al.*, 2006] reflecting the latitudinal structure of the main terdiurnal modes [*Akmaev*, 2001].

[13] A bow-wave structure of small-scale waves observed in nighttime thermospheric densities at 400 km, similar to the one seen in Figure 5, has recently prompted *Forbes et al.* [2008] to suggest that these waves and perhaps the MTM may be at least partially generated in situ by the fast movement of the evening terminator through the thermosphere. Our simulations clearly demonstrate (Figure 3) that the MTM originates in the lower thermosphere from sources possibly connected to the middle and lower atmosphere. A closer examination of Figure 1 also reveals the presence of smaller secondary maxima on some nights between approximately 20:00–21:00 LT as well as in the early morning hours. Similar features have been observed from the ground (J. W. Meriwether, personal communication, 2009). It would be interesting to investigate the origin of these variations and their possible relation to the density waves observed by *Forbes et al.* [2008].

4. Conclusions

[14] WAM appears to be the first comprehensive model to internally generate an MTM of a realistic magnitude in the thermosphere. Initial analysis suggests that the MTM is generated in a chain of dynamical processes that can be traced to the lower thermosphere and possibly even further down to tidal sources in the lower atmosphere. WAM simulations reproduce the salient features of the MTM and exhibit its strong variability. Note that in the present simulations the variability is generated internally by stochastic tropospheric weather processes alone and can only be expected to increase with external forcings modulated by geomagnetic and solar activity.

References

Akmaev, R. A. (2001), Seasonal variations of the terdiurnal tide in the mesophere and lower thermosphere: A model study, *Geophys. Res. Lett.*, *28*, 3817–3820.

Akmaev, R. A., and H.-M. H. Juang (2008), Using enthalpy as a prognostic variable in atmospheric modelling with variable composition, *Q. J. R. Meteorol. Soc.*, *134*, 2193–2197.

Akmaev, R. A., T. J. Fuller-Rowell, F. Wu, J. M. Forbes, X. Zhang, A. F. Anghel, M. D. Iredell, S. Moorthi, and H.-M. Juang (2008), Tidal variability in the lower thermosphere: Comparison of Whole Atmosphere Model (WAM) simulations with observations from TIMED, *Geophys. Res. Lett.*, *35*, L03810, doi:10.1029/2007GL032584.

Bracewell, R. N. (2000), *The Fourier Transform and Its Applications*, 3rd ed., 624 pp., McGraw-Hill, Boston, Mass.

Colerico, M. J., M. Mendillo, C. G. Fesen, and J. Meriwether (2006), Comparative investigations of equatorial electrodynamics and low-to-mid latitude coupling of the thermosphere-ionosphere system, *Ann. Geophys.*, *24*, 503–513.

Faivre, M., J. W. Meriwether, C. G. Fesen, and M. A. Biondi (2006), Climatology of the midnight temperature maximum phenomenon at Arequipa, Peru, *J. Geophys. Res.*, *111*, A06302, doi:10.1029/2005JA011321.

Fesen, C. G. (1996), Simulations of the low-latitude midnight temperature maximum, *J. Geophys. Res.*, *101*, 26,863–26,874.

Forbes, J. M., S. L. Bruinsma, Y. Miyoshi, and H. Fujiwara (2008), A solar terminator wave in thermosphere neutral densities measured by the CHAMP satellite, *Geophys. Res. Lett.*, *35*, L14802, doi:10.1029/2008GL034075.

Fuller-Rowell, T. J. (1981), Three-dimensional, time-dependent model of the thermosphere, Ph.D. thesis, 254 pp., Univ. Coll. London, London.

Fuller-Rowell, T. J., et al. (2008), Impact of terrestrial weather on the upper atmosphere, *Geophys. Res. Lett.*, *35*, L09808, doi:10.1029/2007GL032911.

Harper, R. M. (1973), Nighttime meridional neutral winds near 350 km at low to mid-latitudes, *J. Atmos. Terr. Phys.*, *35*, 2023–2034.

Herrero, F. A., and N. W. Spencer (1982), On the horizontal distribution of the equatorial thermospheric midnight temperature maximum and its seasonal variation, *Geophys. Res. Lett.*, *9*, 1179–1182.

Mayr, H. G., I. Harris, N. W. Spencer, A. E. Hedin, L. E. Wharton, H. S. Porter, J. C. G. Walker, and H. C. Carlson Jr. (1979), Tides and the midnight temperature anomaly in the thermosphere, *Geophys. Res. Lett.*, *6*, 447–450.

Meriwether, J., M. Faivre, C. Fesen, P. Sherwood, and O. Veliz (2008), New results on equatorial thermospheric winds and the midnight temperature maximum, *Ann. Geophys.*, *26*, 447–466.

Spencer, N. W., G. R. Carignan, H. G. Mayr, H. B. Niemann, R. F. Theis, and L. E. Wharton (1979), The midnight temperature maximum in the Earth's equatorial thermosphere, *Geophys. Res. Lett.*, *6*, 444–446.

Sutton, E. K. (2008), Effects of solar disturbances on the thermosphere densities and winds from CHAMP and GRACE satellite accelerometer data, Ph.D. thesis, 162 pp., Univ. of Colo., Boulder.

———————————

R. A. Akmaev, Space Weather Prediction Center, NOAA, W/NP9, 325 Broadway, Boulder, CO 80305, USA. (rashid.akmaev@noaa.gov)

T. J. Fuller-Rowell, H. Wang, and F. Wu, CIRES, University of Colorado, 216 UCB, Boulder, CO 80309, USA.